PERGAMON

International Journal of Solids and Structures 39 (2002) 2401–2417

INTERNATIONAL JOURNAL OF SOLIDS and STRUCTURES

www.elsevier.com/locate/ijsolstr

Determination of effective stress range and its application on fatigue stress assessment of existing bridges ☆

Z.X. Li [a,*], T.H.T. Chan [b], J.M. Ko [b]

[a] College of Civil Engineering, Southeast University, 210018 Nanjing, PR China

[b] Department of Civil and Structural Engineering, The Hong Kong Polytechnic University, Kowloon, Hong Kong

Received 22 August 2001; received in revised form 28 January 2002

Abstract

This paper presents a unified approach on determination of the effective stress range based on equivalent law of strain energy and fatigue damage model, so as to provide an efficient approach for accurately assessing effective fatigue stress of existing bridge under traffic loading. A new theoretical framework to relate variable- and constant-amplitude fatigue is proposed in this paper. Different formulation for calculating effective stress range can be derived by the proposed theory, which include the effective stress range by the root mean square, by Miner's law and a new effective stress range based on the nonlinear fatigue damage model. Comparison of the theoretical results of fatigue damage under the effective stress range of the variable-amplitude stress spectrum and experimental data of fatigue damage under realistic traffic loading has confirmed the validity of the proposed theory. As a way to relate variable-amplitude fatigue data with constant-amplitude data, the effective stress range provides the most convenient way for evaluating fatigue damage under variable-amplitude loading. The proposed theory is then applied to provide an efficient approach for accurately assessing fatigue damage of existing bridges under traffic loading, in which online strain history data measured from bridge structural health monitoring system is available. The proposed approach is applied to evaluate the effective stress range for the purpose of the fatigue analysis of a deck section of a long-span steel bridge—the Tsing Ma Bridge in Hong Kong.

Keywords: Fatigue damage; Variable-amplitude loading; Effective stress range; Continuous damage mechanics; Bridge deck; Traffic load; Strain energy

1. Introduction

Steel bridges are very common in the world, they are expected to be vulnerable to fatigue and fracture-related damage. It is an essential problem to evaluate the accumulative fatigue damage for steel bridges.

☆ The project supported by National Nature Science Foundation of China (50178019) and the Research Grants Council of the Hong Kong SAR Government (B-Q514).

* Corresponding author. Fax: +86-25-771-2719.

E-mail address: zhxli@seu.edu.cn (Z.X. Li).

0020-7683/02/$ - see front matter
PII: S0020-7683(02)00120-8

The problem becomes more complicated if the deterioration condition of an existing steel bridge needs to be considered. In the current approach or code of practice for bridge fatigue design or evaluation (AASHTO, 1989, 1990; BSI, 1982), the deterioration condition, the development of the deterioration and its influence on the structural stress–strain response are all not considered. In fact, in the vicinity of weld, defects such as cracks and voids due to welding and local stress concentration will be developed under durable and cyclic loading. It definitely has the influence on the strain and stress response there, and will generate over-stress in the bridge which again increases the evolution of the local damage. Therefore, it is really necessary to consider the damage evolution and its influence on stress–strain response in the evaluation of fatigue damage for existing steel bridges.

A lot of recent researches on fatigue damage (Fatemi and Yang, 1998; Schijve, 1996) are mainly focused upon two aspects. Firstly, it is the theoretical research on the behavior of fatigue damage and its constitutive modeling, such as the approaches based on crack growth concepts (Miller and Zachariah, 1977; Miller, 1985; Lin and Smith, 1999), the continuous damage mechanics (CDM) models (Shang and Yao, 1999; Chaboche and Lesne, 1988; Lemaitre and Plumtree, 1979) and the energy-based theories (Golos and Ellyin, 1987; Halford, 1966), etc. These fatigue models are advantaged in describing the deterioration on accumulative fatigue process. However they are still on a primary stage to investigate the material specimens in the laboratory and have a long way to go for engineering applications. The second is the research on fatigue analysis method for engineering structures. In this aspect, bridge fatigue behaviors and available approach for evaluating fatigue are studied. Systematical works have been carried out by National Cooperative Highway Research Program (NCHRP) such as Schilling et al. (1978a); Fisher et al. (1980); Fisher et al. (1983) and Moses et al. (1986), in which fatigue behavior of welded steel bridges under variable-amplitude loading was experimentally investigated for different bridge members and different class of weld details. These experimental results are applied to develop the current specifications of bridge fatigue in which S–N curves for components and details grouped into several categories are given according to their fatigue resistance. The Miner's law method used in these guides has the advantages of simplicity combined with mathematical elegance, making them attractive to practicing structural engineers. However, these approaches do not directly associate fatigue damage with physical mechanism such as fatigue crack initiation and growth, and the influence of fatigue damage on local or global stress response was not considered. It has been proved by Zhao and Haldar (1996) and Agerskov and Nielsen (1999) that the tranditional Miner's law is more applicable to the design of new bridges than to the evaluation of the fatigue damage and the remaining life of existing bridges. Therefore, it is really necessary to seek an efficient approach for accurately assessing fatigue of existing steel bridges. This approach should be based on the fatigue theory directly associate damage mechanism on accumulative fatigue process, and should also be easy to apply to bridge fatigue assessment. That is the purpose of this paper.

As a way relating variable- and constant-amplitude fatigue data, the effective stress range provides the most convenient way for bridge applications. In this paper, A new theoretical framework is proposed to relate constant- and variable-amplitude fatigue and derive different formulae for calculating effective stress range. The effective stress range by root mean square (RMS), by Miner's law and a new effective stress range based on the nonlinear fatigue damage model (NFDM) will be obtained in the same way by the proposed theory. The validity of the proposed theory is validated by comparing the theoretical results of fatigue under the effective stress range with the experimental data of fatigue under realistic traffic loading. Then, the proposed theory is applied to provide an efficient approach for accurately assessing effective fatigue stress of existing bridges under traffic loading, in which online strain-time history data measured from bridge structural health monitoring system is available. The application of the proposed approach is carried out for the fatigue analysis of a bridge-deck section of a large steel bridge—the Tsing Ma Bridge in Hong Kong.

2. Effective stress range by strain energy equivalence

Extensive test results showed that variable-amplitude random sequence stress spectrums, such as those occurring in actual bridges, can be conveniently represented by a single constant-amplitude effective stress range that would result in the same fatigue life as the variable-amplitude stress range spectrum. The effective stress range concept can be used directly in the design of critical bridge members or in estimating the remaining fatigue life of existing bridges, and could eventually be incorporated in bridge-design specification (Schilling et al., 1978b).

The effective stress range for a variable-amplitude spectrum is defined as the constant-amplitude stress range that would result in the same fatigue life as the variable-amplitude spectrum. It can be written as:

$$\Delta\sigma_{\mathrm{ef}} = \left[\frac{1}{N_{\mathrm{T}}}\sum_i n_i \Delta\sigma_i^m\right]^{1/m} \tag{1}$$

in which n_i is number of cycles of stress range $\Delta\sigma_i$, $\Delta\sigma_i$ is variable-amplitude stress range, N_{T} is total number of cycles ($=\sum_i n_i$)

If m is taken as 2, $\Delta\sigma_{\mathrm{ef}}$ from the above equation is equal to the RMS of the stress range in the variable-stress spectrum. This effective stress range by RMS was primarily derived from the effective stress range based on Rayleigh distribution (Schilling et al., 1978a) where the best-fit value of correlation factor, C, is taken to be 0.378.

If m is taken as the slope of the constant-amplitude S–N curve for a particular detail under consideration, the equation is equivalent to Miner's law, and for most structural details, m is about 3. The effective stress range thus calculated was derived from the definition of the effective stress range and Miner's law.

In this paper, the effective stress range calculated by RMS, by Miner's law and a new CDM model described later will be derived by a unified theory, which is based on the equivalent law of strain energy density.

Total strain energy density per cycle is written as:

$$\Delta W^{\mathrm{t}} = \Delta W^{\mathrm{e}} + \Delta W^{\mathrm{p}} \tag{2}$$

where ΔW^{p} is a plastic strain energy density that can be neglected in calculation of strain energy since the macro-plastic strain done not occurred on the high-cycle fatigue process of bridge fatigue. The elastic strain energy density, ΔW^{e}, can be written as:

$$\Delta W^{\mathrm{e}} = \frac{1}{2E}\left(\frac{\Delta\sigma}{2} + \sigma_{\mathrm{m}}\right)^2$$

where σ_{m} is the mean stress in a stress cycle.

Under the uniaxial periodic loading, i.e., stress ratio $R = -1$ and the mean stress $\sigma_{\mathrm{m}} = 0$, the elastic strain energy density generated by the constant-amplitude stress cycles and stress amplitude, $\Delta\sigma$, is calculated as:

$$W_1^{\mathrm{e}} = N_{\mathrm{T}}\Delta W^{\mathrm{e}} = \frac{N_{\mathrm{T}}}{2E}\left(\frac{\Delta\sigma}{2}\right)^2 \tag{3}$$

where N_{T} is the total number of cycles.

The elastic strain energy density generated by a block of variable-amplitude stress cycles can be written as:

$$W_2^e = \sum_i \Delta W_i^e = \frac{1}{2E} \sum_i n_i \left(\frac{\Delta \sigma_i}{2} \right)^2 \tag{4}$$

where the contribution of mean stress in each cycle, σ_{mi}, to the strain energy is not considered. The influence of mean stress on fatigue damage could be considered by modifying the stress amplitude when necessary.

Assuming that, the effective stress range for a variable-amplitude spectrum would result in the same fatigue life as the variable-amplitude stress spectrum if and only if the strain energy density generated by the effective stress range is equivalent to that by the variable-amplitude stress spectrum. That is to say, the effective stress range for a variable-amplitude stress spectrum should be derived from the equivalence of Eqs. (3) and (4) as follows:

$$W_1^e = W_2^e \Rightarrow \Delta \sigma_{ef} = \left[\sum_i \frac{n_i}{N_T} \left(\frac{\Delta \sigma_i}{2} \right)^2 \right]^{1/2} \tag{5}$$

where n_i/N_T is the fraction of stress ranges $\Delta \sigma_i$ in the spectrum.

The effective stress range calculated by the above equation is in the same form of that by RMS and given by Eq. (1). It suggests that the effective stress range by RMS for a variable-amplitude stress spectrum satisfies the equivalent law of strain energy. It should be noticed that Eq. (5) is available only when the influence of mean stress σ_{mi} in variable-amplitude stress cycles is quite small to be neglected.

3. Effective stress range based on strain energy with account for fatigue damage effect

In the above section, the deteriorated condition and its influence on fluctuations of stress range are not considered in the calculation of strain energy density. As mentioned in the introduction, fatigue damage in bridge deck, usually appeared at the location of weld or other typical connections, will develop in the process of durable and cyclic loading, and induce stress concentration. This behavior can be well described by the theory of CDM (Kachanov, 1986; Krajcinovic and Lemaitre, 1987; Lemaitre and Chaboche, 1990). In the phenomenological aspect, fatigue damage variable is defined as the ratio of area of fatigue cracks to the original uncracked area. Therefore, damage variable represents a surface density of cracks or other type of discontinuities in the material. $D = 0$ corresponds to the nondamaged or virgin state, and $D = 1$ corresponds to the failure where the volume element considered to be broken into two parts. Generally, $1 > D \geqslant 0$ characterizes the state of damage. Based on this phenomenal description of damage, the constitutive equation of damage material or structure can be obtained by the constitutive law of the virgin material in which the nominal stress is replaced by the effective stress (Lemaitre, 1987). The effective stress or net stress due to damage, $\tilde{\sigma}$, is written as:

$$\tilde{\sigma} = \frac{\sigma}{1 - D} \tag{6}$$

where σ is the nominal stress.

Considering the state of fatigue damage and its influence on strain and stress response, the strain energy density at the effective stress range now can be written as:

$$W_1^e = N_T \Delta W^e = \frac{N_T}{2E} \left(\frac{\Delta \tilde{\sigma}_{ef}}{2} \right)^2 = \frac{N_T}{2E} \left(\frac{\Delta \sigma_{ef}}{2} \right)^2 \left(\frac{1}{1 - D_{ef}} \right)^2 \tag{7}$$

where D_{ef} represents the current fatigue damage due to N_T cycles of the effective stress range $\Delta \sigma_{ef}$. And the strain energy density at the variable-amplitude stress spectrum now can be written as:

$$W_2^{\mathrm{e}} = \frac{1}{2E}\sum_i n_i\left(\frac{\Delta\tilde{\sigma}_i}{2}\right)^2 = \frac{1}{2E}\sum_i n_i\left(\frac{\Delta\sigma_i}{2}\right)^2\left(\frac{1}{1-D_i}\right)^2 \tag{8}$$

where D_i represents the current damage at variable-amplitude stress spectrum.

Based on the equivalent law of strain energy, Eq. (7) is equal to Eq. (8). Substituting Eq. (5), it yields:

$$D_{\mathrm{ef}} = D_i \tag{9}$$

It is suggested that the equivalent law of strain energy will be satisfied for damaged structure if and only if the current state of damage calculated by the effective stress range is equal to that calculated by variable-amplitude stress spectrum. That is to say, considering the state of fatigue damage and its influence on strain energy, the effective stress range for a variable-amplitude spectrum would result in the same fatigue life as the variable-amplitude stress spectrum if and only if the following two conditions are satisfied at the same time:

(a) strain energy density generated by the effective stress range is equivalent to that by the variable-amplitude stress spectrum,
(b) and the calculated damage value based on effective stress range is equivalent to that based on variable-amplitude stress spectrum.

Based on the above principle, different methods of calculating the effective stress range are obtained by use of different fatigue damage model.

3.1. Miner's fatigue model

The effective stress range by Miner's law now can be derived from the theory proposed. According to Miner's linear damage law, the current damage at constant-amplitude cycles with effective stress range is:

$$D_{\mathrm{ef}} = \frac{N_{\mathrm{T}}}{A\,\Delta\sigma_{\mathrm{ef}}^{-m}} \tag{10}$$

And the current damage at variable-amplitude stress spectrum:

$$D_i = \sum_i \frac{n_i}{A\Delta\sigma_i^{-m}} \tag{11}$$

Substituting the above two relations into Eq. (9), the effective stress range by Miner's law is again obtained.

3.2. Fatigue damage model based on continuous damage mechanics

A new effective stress range will be derived by means of the above theory and the fatigue damage model based on CDM.

Based on the theory of thermodynamics and potential of dissipation, a general continuous damage model for high-cycle fatigue problems can be written as a functional of the accumulated plastic or micro-plastic strain, the strain energy density release rate and current state of damage (Krajcinovic and Lemaitre, 1987). The micro-plastic strain, usually neglected in a low-cycle fatigue problem, and its accumulation must be considered when high-cycle fatigue damage occurred in the elastic range, even if macro-plastic strain does not exist. Therefore, the damage evolution equation here is written as (Lemaitre, 1987):

$$\begin{aligned} \dot{D} &= \frac{R_v \sigma_{\mathrm{eq}}^2 \left|\sigma_{\mathrm{eq}} - \bar{\sigma}_{\mathrm{eq}}\right|^{\beta}}{B(1-D)^{\alpha}} \langle \dot{\sigma}_{\mathrm{eq}} \rangle \quad \text{if } \sigma^* \geqslant \sigma_{\mathrm{f}} \\ \dot{D} &= 0 \qquad \text{if } \sigma^* < \sigma_{\mathrm{f}} \end{aligned} \tag{12}$$

where B and β are constants of material, σ_{f} is the stress limit to fatigue, σ_{eq} is an effective stress for taking into account the effect of multiaxial stresses, which could be the maximum of principle stresses (if the influence of fatigue crack closing on fatigue damage is not considered) or Von Mises equivalent stress. And $\bar{\sigma}_{\mathrm{eq}}$ is the mean value of σ_{eq} over a stress cycle. In Eq. (12), the symbol $\langle\ \rangle$ denotes the usual McCauley brackets, $\langle x \rangle = x$ for $x > 0$ and $\langle x \rangle = 0$ for $x < 0$, and σ^* is the damage equivalent stress which, for damage, acts as the Von Mises equivalent stress used in plasticity. And R_v is a triaxiality function to express the influence of the triaxial ratio of the stress state, and in pure bilateral conditions ($h = 1$) this function reduces to:

$$R_v = \left[\frac{\sigma^*}{\sigma_{\mathrm{eq}}}\right]^2 = \frac{2}{3}(1+v) + 3(1-2v)\left[\frac{\sigma_H}{\sigma_{\mathrm{eq}}}\right]^2 \tag{13}$$

Eq. (12) is a general constitutive model for high-cycle fatigue that is valid for any kind of loading. It has to be integrated over time for each cycle if the cycles are different in magnitude of stress range and mean stress. Suppose the stress-time history in a bridge is blocked cyclic history, the block of stress cycles is a unit of variable-amplitude spectrum with N_{T} numbers of stress cycles. The fatigue damage equation is now integrated over time for each cycle in one block of stress cycles, from which the fatigue damage generated by one block of the stress cycles can be derived.

Considering firstly the mean stress $\sigma_{\mathrm{m}} = 0$ for simplicity of the calculation, and neglecting the variation of $(1-D)^{\alpha}$ in the calculation, integrating of Eq. (12) in the case of uniaxial loading for one block of stress cycles yields:

$$\int_D^{D+(\delta D/\delta N_{\mathrm{bl}})} \mathrm{d}D = \sum_{i=1}^{N_{\mathrm{T}}} \int_0^{\sigma_{\mathrm{M}ri}} \frac{\sigma^{\beta+2}}{B(1-D)^{\alpha}}\,\mathrm{d}\sigma \quad \text{for } \bar{\sigma} = \sigma_{\mathrm{m}} = 0 \tag{14}$$

where N_{bl} is the number of blocks and $\sigma_{\mathrm{M}ri}$ is the maximum stress at ith cycle and its value is greater than the stress limit to fatigue.

When $\sigma_{\mathrm{m}} = 0$ the stress amplitude σ_{ar} is equal to the maximum stress σ_{Mr}; the Eq. (14) thus leads to:

$$\frac{\delta D}{\delta N_{\mathrm{bl}}} = \sum_{i=1}^{N_{\mathrm{T}}} \frac{\sigma_{\mathrm{ar}i}^{\beta+3}}{B(1-D)^{\alpha}(\beta+3)} \tag{15}$$

Now, consider the effect of mean stresses by using the equations similar to that of Morrow, or that of Smith et al. (1970):

$$\sigma_{\mathrm{ar}} = (\sigma_{\mathrm{M}}\sigma_{\mathrm{a}})^{1/2} \tag{16}$$

Substituting the above equation into Eq. (15), and since $\sigma_{\mathrm{M}} = \sigma_{\mathrm{a}} + \sigma_{\mathrm{m}}$, it gives:

$$\frac{\delta D}{\delta N_{\mathrm{bl}}} = \frac{1}{B(1-D)^{\alpha}(\beta+3)} \sum_{i=1}^{N_{\mathrm{T}}} [(\Delta\sigma_i + 2\sigma_{\mathrm{m}i})\Delta\sigma_i]^{(\beta+3)/2} \quad \text{for } \sigma_{\mathrm{M}i} \geqslant \sigma_{\mathrm{f}} \tag{17}$$

in which $\sigma_{\mathrm{a}i} = (1/2)\Delta\sigma_i$ has been used.

The above equation gives the fatigue damage rate generated in one block of variable-amplitude stress cycles. The fatigue damage rate generated by the effective stress range is obtained as a special situation of the above equation:

$$\frac{\delta D}{\delta N_{\mathrm{bl}}} = \frac{\Delta\sigma_{\mathrm{ef}}^{\beta+3} N_{\mathrm{T}}}{B(1-D)^{\alpha}(\beta+3)} \tag{18}$$

The damage value in the above equation is the current damage calculated by the effective stress range, while the damage value in Eq. (17) is obviously the one calculated by variable-amplitude stress spectrum. From the condition given by Eq. (9), the effective stress range by CDM fatigue damage model is obtained as follows:

$$\Delta\sigma_{\mathrm{ef}} = \left\{ \sum_i \frac{n_i}{N_{\mathrm{T}}} [(\Delta\sigma_i + 2\sigma_{\mathrm{m}i})\Delta\sigma_i]^{(\beta+3)/2} \right\}^{1/(\beta+3)} \tag{19}$$

The above equation is the same as the effective stress range developed by Miner's law, if the effect of mean stress at each cycle is considered in the same way as in this section, and if the parameter, $\beta + 3$, is identified as the slope of the constant-amplitude S–N curve for a particular connection detail. It suggests that, although the fatigue damage modeled by Miner's law and by CDM damage model follows different rule of damage evolution, they give the similar result on the relation between constant- and variable-amplitude fatigue.

3.3. Nonlinear fatigue damage model

The research on fatigue damage evolution (Krajcinovic and Lemaitre, 1987) has shown that, the parameter α in Eq. (17) is not a constant on the accumulative process of fatigue under variable-amplitude loading. Li et al. (2001a) found that the parameter depends on amplitude of stress range:

$$\alpha = f(\Delta\sigma) \tag{20}$$

and α is called as a nonlinear accumulative parameter of fatigue damage.

The equation of fatigue damage rate generated by a block of variable-amplitude stress cycles is rewritten as:

$$\frac{\delta D}{\delta N_{\mathrm{bl}}} = \frac{1}{B(\beta+3)} \sum_{i=1}^{N_{\mathrm{T}}} \frac{[(\Delta\sigma_i + 2\sigma_{\mathrm{m}i})\Delta\sigma_i]^{(\beta+3)/2}}{(1-D)^{\alpha_i}} \tag{21}$$

in which $\alpha_i = f(\Delta\sigma_i) = k_\sigma \Delta\sigma_i + \alpha_0$ (Li et al., 2001a).

The equation (21) is a nonlinear evolution law of fatigue damage, and an explicit solution of the fatigue damage is difficult to get from Eq. (21). In order to obtain the effective stress range by this nonlinear damage model, the following condition should be satisfied together with Eq. (9):

$$\left(\frac{\delta D}{\delta N_{\mathrm{bl}}}\right)_{\mathrm{ef}} = \left(\frac{\delta D}{\delta N_{\mathrm{bl}}}\right)_i \tag{22}$$

in which the subscripts ef and i outside the parentheses indicate that the values of affected quantities are computed by use of constant-stress range $\Delta\sigma_{\mathrm{ef}}$ or variable-amplitude stress spectrum $\Delta\sigma_i (i = 1, 2, \ldots)$ respectively.

Substituting Eqs. (18) and (21) into the above equation, we have:

$$\frac{\Delta\sigma_{\mathrm{ef}}^{\beta+3}}{(1-D)^{\alpha_{\mathrm{ef}}}} = \sum_i f_{\mathrm{r}i} \frac{[(\Delta\sigma_i + 2\sigma_{\mathrm{m}i})\Delta\sigma_i]^{(\beta+3)/2}}{(1-D)^{\alpha_i}} \tag{23}$$

where $f_{\mathrm{r}i} = n_i/N_{\mathrm{T}}$ is the fraction of stress range $\Delta\sigma_i$.

Then, the effective stress range can be obtained as follows:

$$\Delta\sigma_{\mathrm{ef}} = \left\{ \sum_i f_{\mathrm{r}i} \frac{[(\Delta\sigma_i + 2\sigma_{\mathrm{m}i})\Delta\sigma_i]^{(\beta+3)/2}}{(1-D)^{\alpha_i - \alpha_{\mathrm{ef}}}} \right\}^{1/(\beta+3)} \tag{24}$$

The above equation shows that, the effective stress range given by the above equation is the function of the current value of damage and therefore also the number of blocks:

$$\Delta\sigma_{\mathrm{ef}} = f(D, N_{\mathrm{bl}}) \tag{25}$$

It implies that, the effective stress range by the NFDM is actually constant-amplitude related to the block of stress cycles. That is to say, at a given value of the block number, the effective stress range is a constant; however, it varies with the increase of fatigue damage and the number of blocks. Considering accumulative fatigue damage and its influence on stress response, such a result of effective stress range is quite reasonable.

The equation (24) shows a nonlinear relation between the effective stress range $\Delta\sigma_{\mathrm{ef}}$. And the parameter α_{ef} since it is dependent on $\Delta\sigma_{\mathrm{ef}}$:

$$\alpha_{\mathrm{ef}} = f(\Delta\sigma_{\mathrm{ef}}) = k_\sigma \Delta\sigma_{\mathrm{ef}} + \alpha_0 \tag{26}$$

For the reason of simplicity, the effective stress range can be calculated step by step with the help of increment method, in which the current damage D, kth increment, is calculated by the value of the effective stress range at the $(k-1)$th increment, and α_{ef} at kth increment is replace by its value at the $(k-1)$th increment. Eq. (24) is thus rewritten as:

$$\Delta\sigma_{\mathrm{ef}}^k = \left[\sum_i f_{ri} \frac{[(\Delta\sigma_i + 2\sigma_{\mathrm{m}i})\Delta\sigma_i]^{(\beta+3)/2}}{(1-D^k)^{\alpha_i - \alpha_{\mathrm{ef}}^{k-1}}} \right]^{1/(\beta+3)} \tag{27}$$

where $\alpha_{\mathrm{ef}}^{k-1} = f(\Delta\sigma_{\mathrm{ef}}^{k-1})$ and D^k is calculated by use of the following equation:

$$D^k = 1 - \left[\left(1 - D^{k-1}\right)^{\alpha+1} - \frac{N_{\mathrm{T}} \Delta N_{\mathrm{bl}}^k (\alpha+1)}{B(\beta+3)} \left(\Delta\sigma_{\mathrm{ef}}^{k-1}\right)^{\beta+3} \right]^{1/(\alpha+1)} \tag{28}$$

where $\Delta N_{\mathrm{bl}}^k = N_{\mathrm{bl}}^k - N_{\mathrm{bl}}^{k-1}$, and $\alpha = \alpha_{\mathrm{ef}}^{k-1}$. The above equation is derived from Eq. (18) at the initial conditions $D = D^{k-1}$ when $N_{\mathrm{bl}} = N_{\mathrm{bl}}^{k-1}$; and $D = D^k$ when $N_{\mathrm{bl}} = N_{\mathrm{bl}}^k$.

The identification of the coefficients B, β and α in the model needs the Woehler curve for uniaxial periodic fatigue and the measurement of damage derived by means of strain controlled fatigue test.

4. Comparison of theoretical results and experimental data

To determine whether the fatigue life evaluated by the effective stress range is close to that by the variable-amplitude data, it is necessary to compare theoretical results of fatigue life calculated by the effective stress range with experimental fatigue data under variable-amplitude loading. Schilling et al. (1978a) presented the comparison for the effective stress range by RMS and Miner methods. In their work, the effective stress range for the variable-amplitude data was compared with stress range for the constant-amplitude data. And their fatigue experimental data was obtained by testing bridge members under simulated traffic loading based on the number and variation of truck loading in an actual bridge. The frequency of occurrence used in their tests was designed by four factorials: $S_{\mathrm{rd}}/S_{\mathrm{rm}} = 0.00, 0.25, 0.50, 1.00$ (S_{rm} is the modal stress range and S_{rd} is the dispersion or variation of the stress range in the spectrum), in which $S_{\mathrm{rd}}/S_{\mathrm{rm}} = 0.00$ corresponds to constant-amplitude loading.

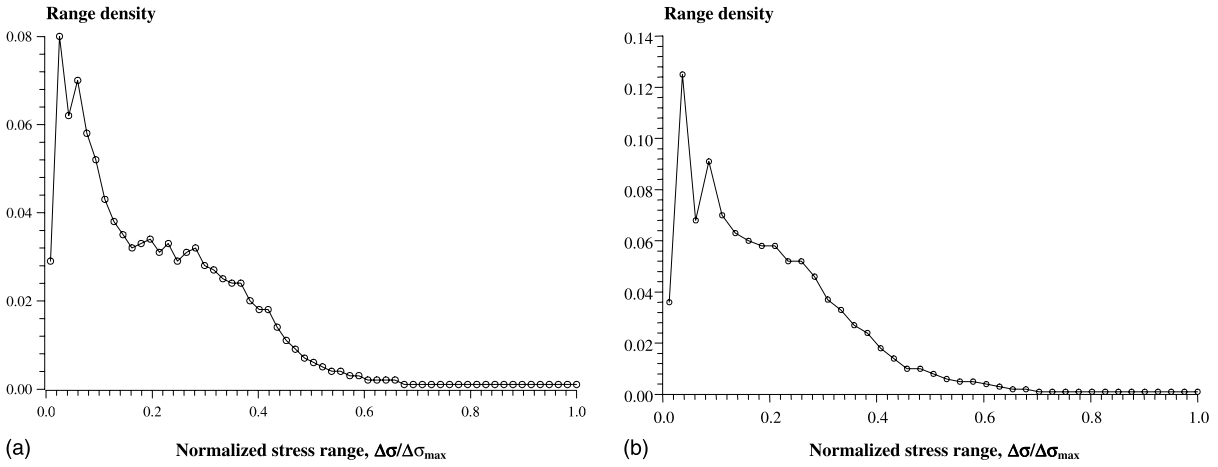

Fig. 1. Density of rain-flow counted stress ranges for load history from (a) strain gauge no. 1 and (b) strain gauge no. 5.

In this section, the comparison will be carried out for the effective stress range by Miner and the NFDM methods, in which the experimental data of fatigue under more realistic fatigue loading is available. The fatigue tests by Nielsen et al. (1997) have been carried out on plate specimens with transverse attachments. Since traffic loading is the dominant variable-amplitude loading on steel bridge decks, the variable-amplitude loading used in their fatigue tests had been determined from strain gauge measurements on the orthotropic steel deck structure of a bridge in Denmark. Fig. 1(a) and (b) show the range density of the rain-flow counted stress ranges for the load history measured by strain gauge no. 1 and no. 5 respectively.

The load history resulting from the measurement from strain gauge no. 1 is primarily in the tension area (Nielsen et al., 1997). It appears from the load history that approximately $5/6$ of the stresses is in tension and approximately $1/6$ is in compression. Thus, it seems reasonable to compare the results obtained in this test series with calculated results by use of the developed fatigue model with identified model parameter from the constant-amplitude test series at stress ratio $R = -1/5$. While the load history based on the measurements from strain gauge no. 5 (Nielsen et al., 1997) is almost equal in tension and compression. The maximum stresses in tension and compression are practically the same for this load history. This means that the results of the test series with the load history based on strain gauge no. 5 should be compared with calculated results by use of the developed fatigue model with identified model parameter from the constant-amplitude test series at stress ratio $R = -1$.

Fig. 2(a) and (b) show S–N diagrams plotted by the effective stress range calculated by NFDM and Miner methods respectively. Data points for both constant- and variable-amplitude tests are also plotted, in which the data points for variable-amplitude loading measured from strain gauges no. 5 (with stress ratio $R = -1$) have been transformed by the NFDM and Miner methods respectively.

Fig. 3(a) and (b) show S–N diagrams plotted by the effective stress range calculated by NFDM and Miner methods respectively. Data points for both constant- and variable-amplitude tests are also plotted, in which the data points for variable-amplitude loading measured from strain gauges no. 1 (with stress ratio $R = -1/5$) have been transformed by the NFDM and Miner methods respectively. Table 1 gives fatigue damage model parameters used in above theoretical calculations.

It can be seen that the theoretical results of the effective stress range by NFDM and Miner methods are well fitted with the experimental data in statistical sense for both constant- and variable-amplitude test series at stress ratio $R = -1$. However, a relative large difference between the theoretical results and

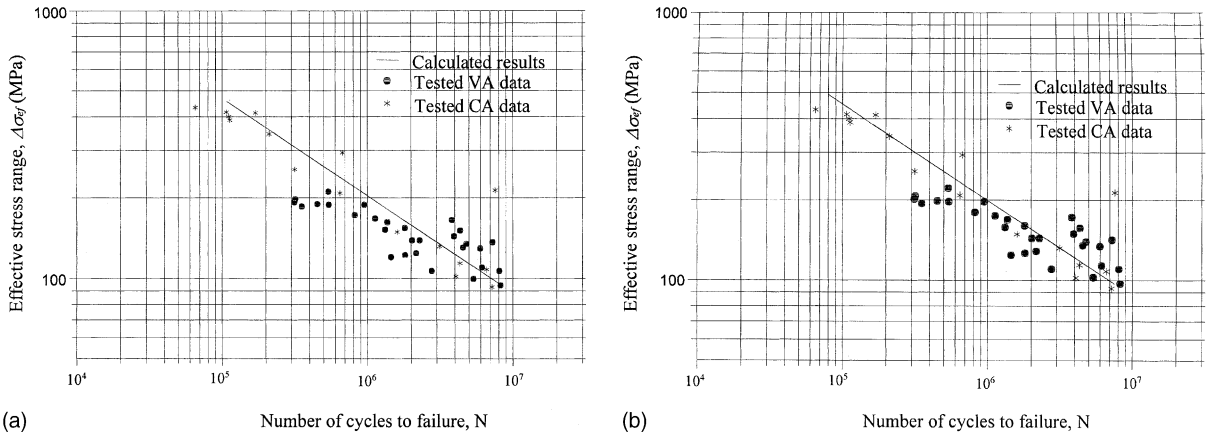

Fig. 2. Effective stress range vs. fatigue life for small plate specimen at VA load history from strain gauge no. 5 and CA load, $R = -1$ by (a) NFDM and (b) Miner.

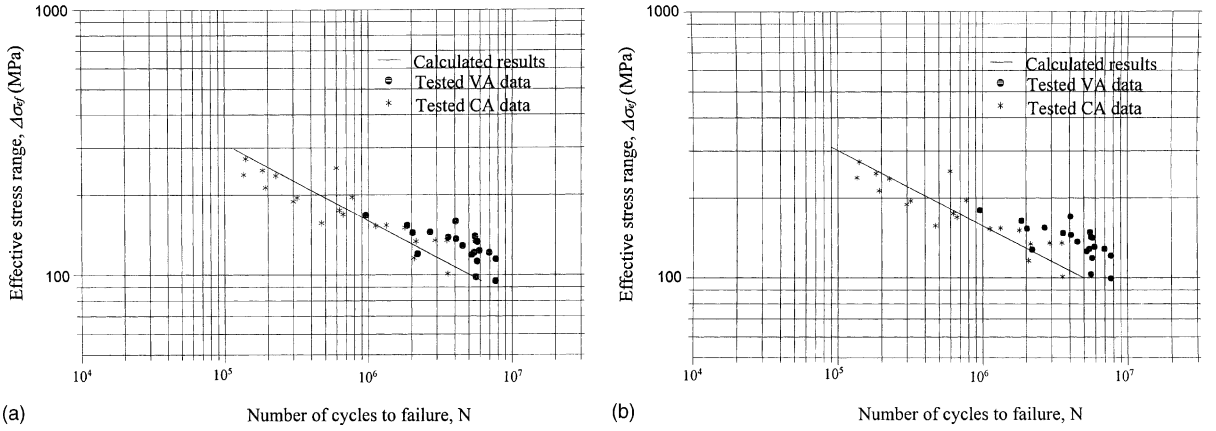

Fig. 3. Effective stress range vs. fatigue life for small plate specimen at VA load history from strain gauge no. 1 and CA load, $R = -1/5$ by (a) NFDM and (b) Miner.

Table 1
Fatigue damage model parameters used in theoretical calculation

Stress ratio	$\beta + 3$	$k_\alpha/B(\beta + 3)$	$(\alpha_0 + 1)/B(\beta + 3)$
$R = -1$	2.796	-1.352×10^{-17}	2.014×10^{-14}
$R = -1/5$	3.545	-0.545×10^{-17}	3.858×10^{-14}

variable-amplitude data is observed for test series at stress ratio $R = -1/5$. It is considered to be reasonable since the mean stress here is not equal to zero while the effect of mean stress in each cycle of the stress spectrum is not included in the calculation for the reason of simplicity.

5. Efficient approach of bridge fatigue analysis and its application

The effective stress range provides a link between the variable-amplitude fatigue loading that actually occur on bridges and the constant-amplitude fatigue data and allowable-stress ranges that are commonly used in fatigue design and evaluation of bridges. It will be applied to fatigue evaluation for bridges with online health monitoring data in this section.

5.1. Approach of fatigue analysis under blocked cycles of traffic loading

Fatigue analysis and life prediction of the bridge-deck section for bridges with online health monitoring data can be carried out by use of the strain-time history data measured by the health monitoring system. The strain-time history data have been shown to be approximately a block repeated cycles in which the cycles are daily repeated (Li et al., 2001b). Therefore, it can be represented by a blocked repeated cycles. The stress spectrum of the block, called the representative block of cycles, can be obtained by rain-flow counting cycles of the strain history and statistical analysis on daily samples of strain spectrum. The approach of fatigue analysis for deck sections of bridges with the health monitoring system was provided by Li et al. (2001a). Based on the proposed theory, the approach can be further improved by use of the effective stress range. The effective stress range for the variable-amplitude spectrum at a given location is a quantitative description of fatigue stress and fatigue resistance (class of the welded details, fatigue stress limit, etc.) of the member under consideration. Therefore it can be considered as a representative value of fatigue behavior at the location. On this point of view, the fatigue analysis of bridge-deck sections should be carried out only for the critical location on the section where the effective stress range is comparatively large at the section. The improved approach based on this idea is as shown in Fig. 4, in which the fatigue analysis is carried out for the critical location instead of being done for each of the locations. The most critical location is determined by the value of the effective stress range.

5.2. Variation and distribution of effective stress range in a bridge-deck section

In this section, the approach proposed above is applied to evaluate the effective stress range of the bridge-deck section for the purpose of fatigue analysis of Tsing Ma Bridge.

The Tsing Ma Bridge of 2.2 km total length with a main span of 1377 m is the longest suspension bridge in the world carrying both highway and railway traffic. As the main part of the Lantau Link, a combined highway and railway transport connection between Tsing Yi Island and Lantau Island, it forms an essential part of the transport network for the new airport of Hong Kong. The Bridge was commissioned on May 22, 1997. In order to ensure user comfort and bridge safety, a structural monitoring system has been devised by the Highways Department of the Hong Kong SAR Government (Lau and Wong, 1997) to monitor the integrity, durability and reliability of the bridge. This monitoring system comprises a total of approximately 900 sensors, including accelerometers, strain gauges, displacement transducers, level sensors, anemometers, temperature sensors and weigh-in-motion sensors, installed permanently on the bridges and the data acquisition and processing system. The strain gauges which were installed to measure strain in bridge-deck sections are shown in Fig. 5. The locations of strain gauges installed in the Tsing Ma Bridge include rail track sections at CH 24662.50, bridge-deck trough section at CH 24664.75 and deck at tower and rocker bearing links at CH 23623.00. The most critical parts of the cross frames for fatigue damage have been identified during the design of the WASHMS. Fig. 6 shows locations of all strain gauges, including two sets of rosette strain gauges and 42 linear strain gauges, in the cross frame at CH 24662.5. In the figure, the strain gauge numbered by "SSTLN-nn" and "SSTLS-nn" represent the linear strain gauge set at the north and south of the cross frame respectively, and "SPTLN-nn" and "SPTLS-nn" represent a pair of linear strain gauges set at the north and south of the cross frame respectively. While "SRTLN-01" and

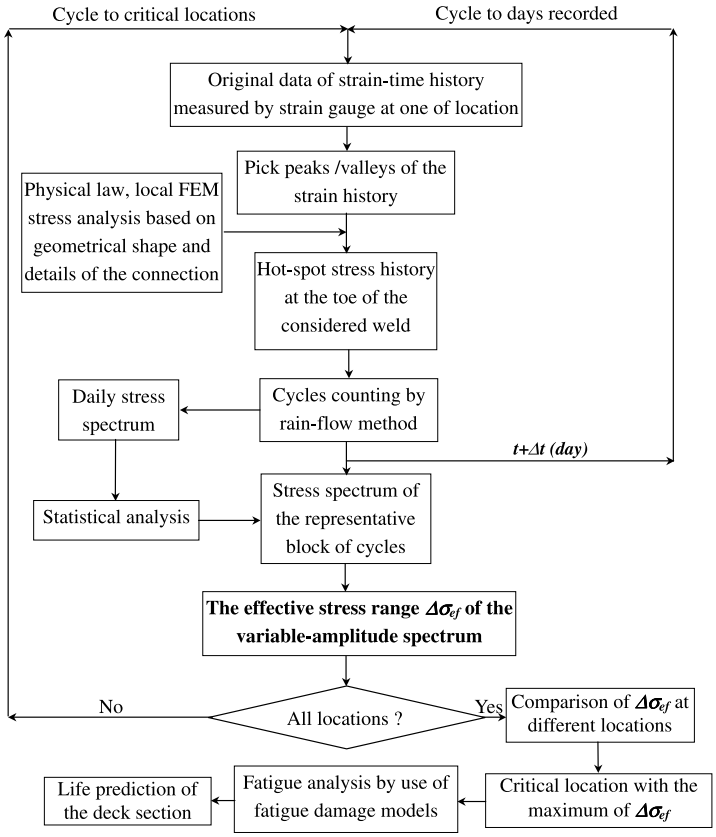

Fig. 4. A flow chart of the approach for fatigue analysis of bridge deck sections.

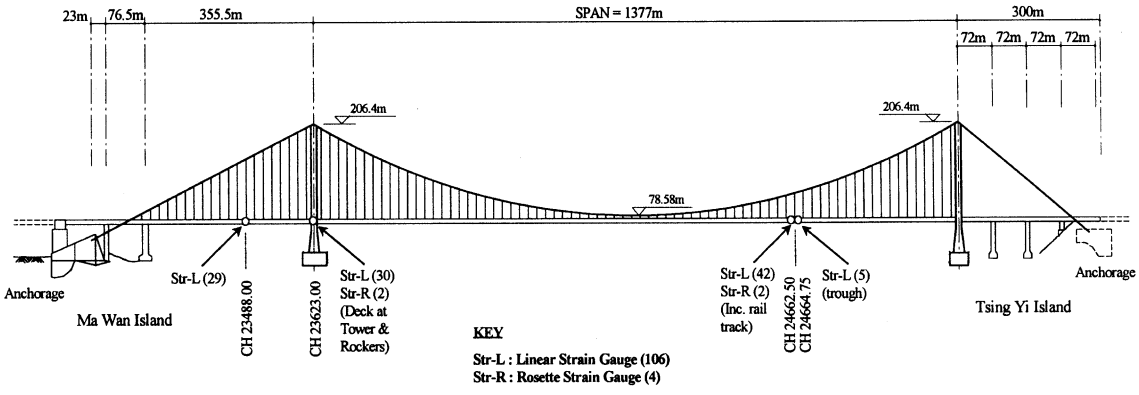

Fig. 5. Strain gauges layout of the Tsing Ma Bridge.

"SRTLS-01" are two set of rosette strain gauges in the north and south respectively. The location of each strain gauge in the cross frame can be better found from Table 2 together with Fig. 6. Strain histories measured by these strain gauges have been recorded since the bridge commissioned on May 22, 1997. As an

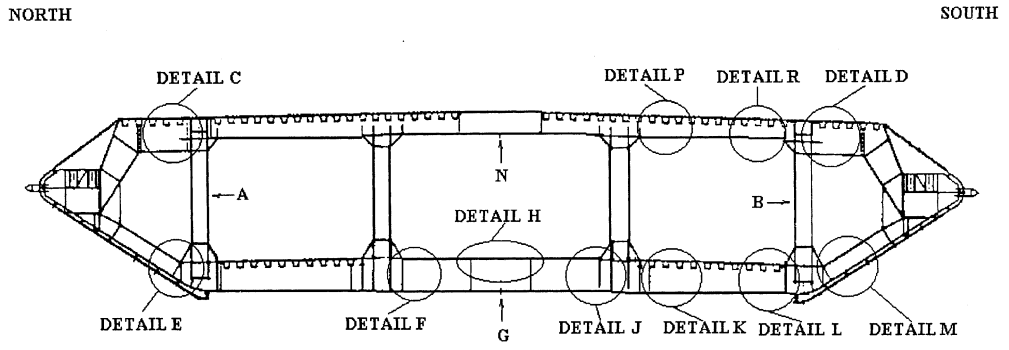

(a) Strain gauge location in the cross frame at CH 24662.50

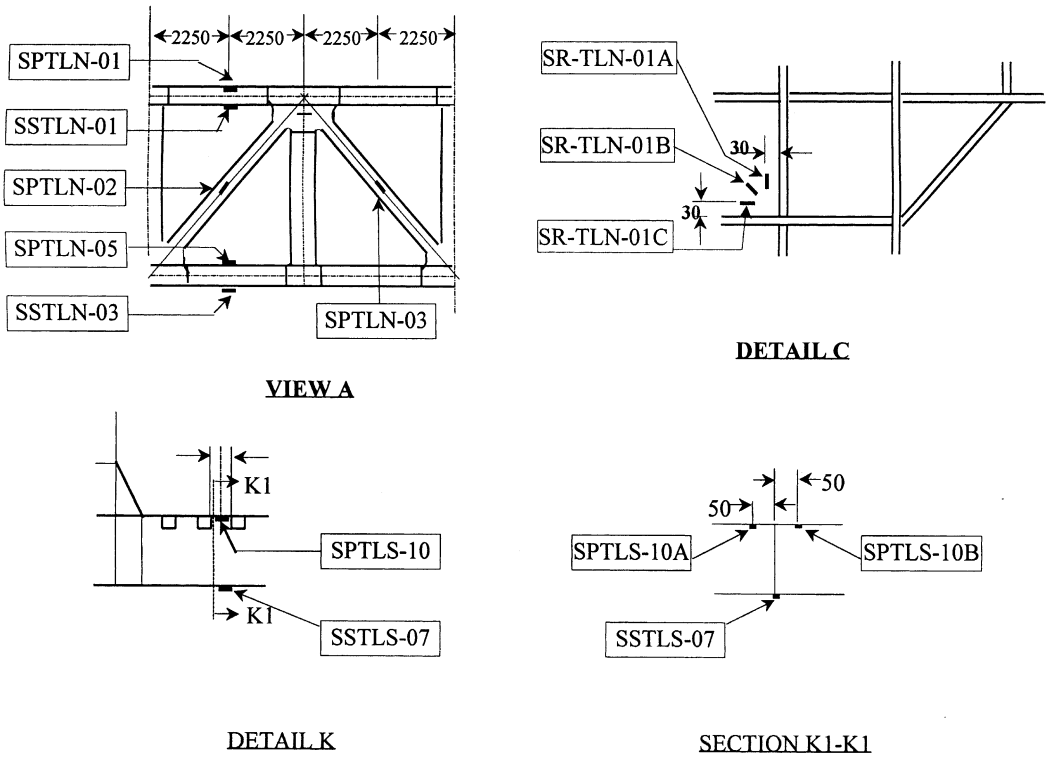

(b) Some figures for details and views in the figure (a)

Fig. 6. Location of strain gauges in cross frame at CH 24662.50 in TMB (Drawing No. P18/C9/E/TM/04/287, 1998).

example to show the nature of strain-time history, the strain-time history measured by the strain gauge "SSTLS-01" and "SPTLS-09" over an hour is shown in Fig. 7(a) and (b) respectively. The strain histories over a longer time period have been discussed and then the stress spectrum was obtained by use of rain-flow counting in our previous works (Li et al., 2001a).

Table 2
Distribution of the effective stress range and locations of related strain gauge inside the cross frame at CH 24662.5

No. of gauge	Location	$\Delta\sigma_{ef}/\Delta\sigma_0$*	No. of gauge	Location	$\Delta\sigma_{ef}/\Delta\sigma_0$	No. of gauge	Location	$\Delta\sigma_{ef}/\Delta\sigma_0$
SSTLN-01	View A	**1.00**	SSTLS-01	View B	0.33	SPTLS-01	View B	0.39
SSTLN-02	Detail E	0.54	SSTLS-02	Detail P	0.58	SPTLS-02	View B	0.99
SSTLN-03	View A	0.54	SSTLS-03	Detail R	0.35	SPTLS-03	View B	0.78
SSTLN-04	Detail F	0.48	SSTLS-04	Detail J	0.38	SPTLS-04	Detail N	–
SSTLN-05	Detail F	0.51	SSTLS-05	Detail J	**1.52**	SPTLS-05	Detail N	–
SSTLN-06	Detail F	0.34	SSTLS-06	Detail J	0.14	SPTLS-06	Detail P	0.15
SPTLN-01	View A	0.58	SSTLS-07	Detail K	0.47	SPTLS-07	Detail R	0.13
SPTLN-02	View A	0.67	SSTLS-08	Detail L	0.39	SPTLS-08	View G	–
SPTLN-03	View A	0.54	SSTLS-09	View B	–	SPTLS-09	View G	**1.73**
SPTLN-04	Detail E	0.27	SSTLS-10	Detail M	0.11	SPTLS-10	Detail K	0.36
SPTLN-05	View A	0.66	SSTLS-11	Detail H	0.30	SPTLS-11	Detail L	0.39
			SSTLS-12	Detail H	**1.11**	SPTLS-12	View B	0.70
SRTLN-01	Detail C		SSTLS-13	Detail H	0.65	SPTLS-13	Detail M	0.36
			SSTLS-14	Detail H	0.99	SPTLS-14	Detail H	**1.12**
SRTLS-01	Detail D					SPTLS-15	Detail H	0.77
						SPTLS-16	Detail H	0.66
						SPTLS-17	Detail H	0.89

* $\Delta\sigma_0$ is the effective stress range at the location of the strain gauge *"SSTLN-01"*.
– Strain data failed to be recorded here.

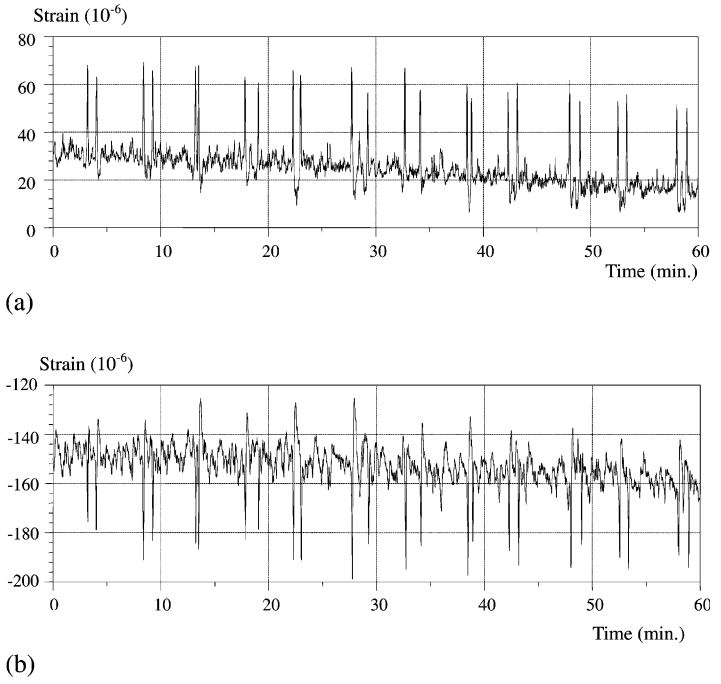

Fig. 7. Strain-time history in an hour at (a) the location "SSTLN-01" and (b) "SPTLS-09".

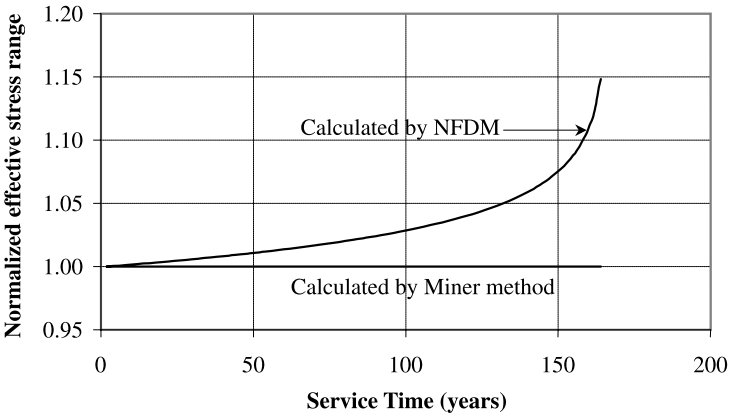

Fig. 8. Variation of the effective stress range with respect to the service time of the bridge.

The effective stress range at the location of the strain gauge "SSTLN-01", calculated by using NFDM and Miner method respectively, is now carefully studied. The variation of the calculated effective stress range with the increase of service time in years for the bridge is shown in Fig. 8. It can be seen that, the effective stress range calculated by NFDM increases with the increase of service time, which is turn increases with the increase of accumulated fatigue damage, while that calculated by Miner method maintains its value as that at the beginning of service. Obviously, the result obtained by NFDM is more close to the actual situation of the fatigue occurred in bridges. It should also be noted that the effective stress range calculated by NFDM has a very small variation at the beginning of service. Therefore it is valid and also efficient to calculate the effective stress range by Miner method at the initial stage of service when the fatigue damage in the bridge is very small, since the calculation of the effective stress range by NFDM is complicated than that by Miner method.

The distribution of the effective stress range at each location of strain gauges is listed in Table 2. The effective stress range at each location of linear strain gauge is calculated by using Eq. (19) where the coefficient $(\beta + 3)$ is simply taken as the same value for all welded connections, and the calculation for the two rosette strain gauges are not included. The distribution of the effective stress range is given by a normalized ratio of $\Delta\sigma_{ef}/\Delta\sigma_0$ where $\Delta\sigma_0$ is the value of effective stress range at the location of the strain gauge "SSTLN-01". It is observed that, several critical locations of fatigue are found at "SSTLN-01" on the Kowloon bound and "SSTLS-05", "SSTLS-12", "SPTLS-09" and "SPTLS-14" on the Airport bound respectively where the effective stress range has a comparatively large value.

Now it is clear that fatigue damage assessment for the deck section CH 24662.5 of the Tsing Ma Bridge should be carried out for the weld connections near the strain gauges "SSTLN-01" on the Kowloon bound and "SSTLS-05", "SSTLS-12", "SPTLS-09" and "SPTLS-14" on the Airport bound respectively. The assessment of fatigue damage and the prediction of residual service life can be made by Miner's law or NFDM based on CDM. Details of the calculation may be found in our previous work on fatigue damage model and fatigue analysis of bridge-deck sections (Chan et al., 2001; Li et al., 2001b). The critical location of the deck section of the Tsing Ma Bridge will be one of those locations with a comparable large value of the effective stress range. In the deck section at CH 24662.5, the critical location will be one of locations of "SSTLN-01", "SSTLS-05", "SSTLS-12", "SPTLS-09" and "SPTLS-14", as shown in Fig. 6. The effective stress range reaches its maximum at "SPTLS-09" which is installed at lower bracing of the cross frame underneath the bridge and mass transit railway (MTR). This result suggests that the accumulative fatigue of the deck section may be dominated by the rail traffic loading.

6. Conclusions

The present work proposed a theoretical framework for the determination of the effective stress range based on equivalent law of strain energy and fatigue damage model, an efficient approach for accurately assessing effective fatigue stress range of existing bridges under traffic loading is then presented based on the proposed theory. The following specific conclusions can be obtained from the present study:

- The proposed theory on the determination of the effective stress range provides a unified approach to derive different formulation for the calculation of the effective stress range for a variable-amplitude spectrum. It is based on the equivalence of strain energy and fatigue damage. The theory leads to a new formulation for the determination of the effective stress range with respect to the nonlinear fatigue damage model, which allows the fatigue damage and its influence on the state of stress to be considered in the calculation of the effective stress range.
- The effective stress range for a variable-amplitude stress spectrum, as a way relating variable-amplitude fatigue data to constant-amplitude data, provides the most convenient way for fatigue assessment of bridges under actual traffic loading. The comparison of the theoretical and the experimental results for fatigue life of an existing under real traffic loading has confirmed the validity of the proposed method.
- The calculated result of the effective stress range by NFDM is more close to the actual situation of the fatigue damage developed in bridges. It is valid and also efficient to calculate the effective stress range by Miner method instead of NFDM method when the bridge is new since the difference between the results obtained by these two methods is very small at the early stage of service. For an old bridge subject to a long history of accumulative fatigue, the significant difference between the effective stress range derived by NFDM and Miner method would be expected.
- The effective stress range would be a useful tool for preliminary estimation of the critical location of fatigue damage. Based on the calculated results on the fatigue analysis of the Tsing Ma Bridge, it could be concluded that the critical location of a deck section should be one of those locations where the effective stress range for the variable-amplitude spectrum measured at these locations has a comparatively large value. These locations should be the targeted positions for further fatigue damage evaluations and nondestructive inspections.

Acknowledgements

This research is sponsored by National Nature Science Foundation of China (Project Code: 50178019) and the Research Grants Council of the Hong Kong SAR Government (Project Code: B-Q514), which are gratefully acknowledged. The writers also wish to thank the Highways Department of the Hong Kong SAR Government for providing the data measured by the long-term structural health monitoring system, the relevant design drawings and documents. Special thanks should be given to Dr. C.K. Lau, Dr. K.Y. Wong, Mr. Kenneth Chan and Mr. Brian Wong of the Highways Department for their valuable supports throughout the project.

References

Agerskov, H., Nielsen, J.A., 1999. Fatigue in steel highway bridge under random loading. Journal of Structural Engineering, ASCE 125, 152–162.

AASHTO, 1989. Guide Specifications for Fatigue Design of Steel Bridges. American Association of State Highway and Transportation Officials, Washington, DC, USA.

AASHTO, 1990. Guide Specifications for Fatigue Evaluation of Existing Steel Bridges. American Association of State Highway and Transportation Officials, Washington, DC, USA.

BSI, 1982. BS5400: Part 10, Code of Practice for Fatigue.

Chaboche, J.L., Lesne, P.M., 1988. A non-linear continuous fatigue damage model. Fatigue and Fracture of Engineering Materials and Structures 11 (1), 1–7.

Chan, T.H.T., Li, Z.X., Ko, J.M., 2001. Fatigue analysis and life prediction of bridge with health monitoring data Part II: Applications. International Journal of Fatigue 23 (1), 55–64.

Drawing No. P18/C9/E/TM/04/287, 1998. Contract No. HY/93/09, Lantau Fixed Crossing, Electrical & mechanical Services.

Fatemi, A., Yang, L., 1998. Cumulative fatigue damage and life prediction theories: a survey of the state of the art for homogeneous materials. International Journal of Fatigue 20 (1), 9–34.

Fisher, J.W., et al., 1980. Fatigue behavior of full-scale welded bridge attachments. NCHRP Report 227, National Academy Press, Washington DC.

Fisher, J.W., et al., 1983. Steel bridge members under variable amplitude long life fatigue loading. NCHRP Report 267, National Academy Press, Washington DC.

Golos, K., Ellyin, F., 1987. Generalization of cumulative damage criterion to multilevel cyclic loading. Theoretical and Applied Fracture Mechanics 7, 169–176.

Halford, G.R., 1966. The energy required for fatigue. Journal of Materials 1 (1), 3–18.

Kachanov, L.M., 1986. Introduction to Continuum Damage Mechanics. Martinus Nijhoff, Dordricht.

Krajcinovic, D., Lemaitre, J., 1987. Continuous Damage Mechanics: Theory and Applications. Springer, Vienna.

Lau, C.K., Wong, K.Y., 1997. Design construction and monitoring of the three key cable-supported bridges in Hong Kong. In: Lee, P.K.K., Balkema, A.A. (Eds.), Structures in the New Millennium. Rotterdam, Netherlands, pp. 105–115.

Lemaitre, J., 1987. Formulation and identification of damage kinetic constitutive equations. In: Continuous Damage Mechanics: Theory and Applications. Springer, Vienna, pp. 37–90.

Lemaitre, J., Chaboche, J.L., 1990. Mechanics of Solid Materials. Cambridge University Press, Cambridge, UK.

Lemaitre, J., Plumtree, A., 1979. Application of damage concepts to predict creep-fatigue failure. Journal of Engineering Materials and Technology, Transactions of the ASME 101, 284–293.

Li, Z.X., Chan, T.H.T., Ko, J.M., 2001a. Fatigue analysis and life prediction of bridge with health monitoring data Part I: Methodology and strategy. International Journal of Fatigue 23 (1), 45–53.

Li, Z.X., Chan, T.H.T., Ko, J.M., 2001b. A nonlinear damage model for fatigue analysis of bridges under traffic loading and its application. Theoretical and Applied Fracture Mechanics 35 (1), 81–91.

Lin, X.B., Smith, R.A., 1999. Finite element modelling of fatigue crack growth of surface cracked plates Part III: Stress intensity factor and fatigue crack growth life. Engineering Fracture Mechanics 63 (5), 541–556.

Miller, K.J., Zachariah, K.P., 1977. Cumulative damage laws for fatigue crack initiation and stage I propagation. Journal of Strain Analysis 12 (4), 262–270.

Miller, K.J., 1985. Initiation and growth rates of short fatigue cracks. In: Fundamentals of Deformation and Fracture. Eshelby Memorial Symposium, Cambridge University Press, Cambridge, UK, pp. 477–500.

Moses, F., Schilling, C.G., et al., 1986. Fatigue evaluation procedures for steel bridge. NCHRP Report 299, National Academy Press, Washington DC.

Nielsen, J.A., Agerskov, H., Vejrum, T., 1997. Fatigue in steel highway bridges under random loading, Rep. No. R 15, Technical University of Denmark, Lyngby, Denmark.

Schijve, J., 1996. Predictions on fatigue life and crack growth as an engineering problem, a state of the art survey. In: Fatigue 96, vol. 2. Pergamon, Oxford, pp. 1149–1164.

Schilling, C.G., et al., 1978a. Fatigue of welded steel bridge members under variable-amplitude loadings. NCHRP Report 188, National Academy Press, Washington DC.

Schilling, C.G. et al., 1978b. New method for fatigue design of bridges. Journal of the Structural Division ASCE 104 (ST3), 425–438.

Shang, D.G., Yao, W.X., 1999. A nonlinear damage cumulative model for uniaxial fatigue. International Journal of Fatigue 21, 187–194.

Smith, K.N., Watson, P., Topper, T.H., 1970. A stress–strain function for the fatigue of metals. Journal of Materials, ASTM 5 (4), 767–778.

Zhao, Z.W., Haldar, A., 1996. Bridge fatigue damage evaluation and updating using non-destructive inspections. Engineering Fracture Mechanics 53 (5), 775–788.